NANO MICRO small
www.small-journal.com

Liquid Crystalline Networks toward Regenerative Medicine and Tissue Repair

Daniele Martella, Paolo Paoli, Josè M. Pioner, Leonardo Sacconi, Raffaele Coppini, Lorenzo Santini, Matteo Lulli, Elisabetta Cerbai, Diederik S. Wiersma, Corrado Poggesi, Cecilia Ferrantini, and Camilla Parmeggiani**

The communication reports the use of liquid crystalline networks (LCNs) for engineering tissue cultures with human cells. Their ability as cell scaffolds for different cell lines is demonstrated. Preliminary assessments of the material biocompatibility are performed on human dermal fibroblasts and murine muscle cells (C2C12), demonstrating that coatings or other treatments are not needed to use the acrylate-based materials as support. Moreover, it is found that adherent C2C12 cells undergo differentiation, forming multinucleated myotubes, which show the typical elongated shape, and contain bundles of stress fibers. Once biocompatibility is demonstrated, the same LCN films are used as a substrate for culturing human induced pluripotent stem cell-derived cardiomyocites (hiPSC-CMs) proving that LCNs are capable to develop adult-like dimensions and a more mature cell function in a short period of culture in respect to standard supports. The demonstrated biocompatibility together with the extraordinary features of LCNs opens to preparation of complex cell scaffolds, both patterned and stimulated, for dynamic cell culturing. The ability of these materials to improve cell maturation and differentiation will be developed toward engineered heart and skeletal muscular tissues exploring regenerative medicine toward bioartificial muscles for injured sites replacement.

Liquid crystalline materials have their greater development in display fabrication research field, resulting in the accurate optimization on their optical and dielectric properties. However, different fields took advantages of many peculiar properties of liquid crystals (LC) for their progress. In particular, their responsiveness to different external stimuli was exploited to selectively control different properties in photonic devices[1,2] or robotic actuators[3–5] and, very recently, also in biological application.[6] In this field, researches were mainly focused on the aggregation of lyotropic liquid crystals in water as medium to encapsulate, transport, and release drugs,[7] while the hydrophobic nature of the common mesogens discourages the application of thermotropic LC in biology.

On the other hand, liquid crystalline mesophases resemble the cellular organization of many human tissues, such as the muscular one, and the exploration of LC polymers as scaffolds for cell growth has recently started.[8,9] Many cell behaviors are strictly connected with cell alignments,[10] and different approaches to engineer in vitro cell alignment has received an increasing interest, especially regarding mechanical loading, topographical patterning, and surface chemical treatment.[11] Liquid crystalline elastomers (LCE) and liquid crystalline networks (LCN) represent ideal materials to integrate these different cell alignment technologies. In fact, such polymers are able to support stress and to change their shape reversibly by application of one of the external stimuli able to induce a liquid crystalline to isotropic phase transition.[12,13] The above mentioned material behavior recently attracted researcher attention resulting in the development of a series of cholesterol-based LCE as porous 3D scaffolds for human

Dr. D. Martella, Dr. L. Sacconi, Prof. D. S. Wiersma, Dr. C. Parmeggiani
European Laboratory for Non-Linear Spectroscopy
via N. Carrara 1, Sesto F. No. 50019, Italy
E-mail: Camilla.parmeggiani@lens.unifi.it
Dr. P. Paoli, Dr. M. Lulli
Dipartimento di Scienze Biomediche
Sperimentali e Cliniche "Mario Serio"
Università degli Studi di Firenze
Viale Morgagni 50, Firenze 50134, Italy
Dr. J. M. Pioner, Prof. C. Poggesi, Dr. C. Ferrantini
Dipartimento di Medicina Sperimentale e Clinica
Università degli Studi di Firenze
Viale Morgagni 63, Firenze 50134, Italy
E-mail: cecilia.ferrantini@unifi.it
Dr. L. Sacconi, Dr. C. Parmeggiani
CNR-INO
via Nello Carrara 1, Sesto F. No. 50019, Italy
Dr. R. Coppini, L. Santini, Prof. E. Cerbai
Dipartimento di Neuroscienze
Psicologia, Area del Farmaco e Salute del Bambino
Università degli Studi di Firenze
Viale Pieraccini, 6-50139 Firenze, Italy
Prof. D. S. Wiersma
Istituto Nazionale di Ricerca Metrologica (INRiM)
Torino 10135, Italy
The ORCID identification number(s) for the author(s) of this article can be found under https://doi.org/10.1002/smll.201702677.

DOI: 10.1002/smll.201702677

myoblast and dermal fibroblast seeding[14] and polysiloxane-based LCEs as stimulated cell scaffolds.[15]

One of the most versatile techniques to prepare LCEs and LCNs is photopolymerization of acrylate-based mesogens.[13,16] The peculiar characteristic of the resulting class of polymers can be exploited and represent an adding value in cell growth experiments.[17] First, they can be simply patterned by lithographic technique,[18,19] to create different 3D surfaces for optimized cell alignment.[20] Furthermore, the presence of commercially available monomers and the possibility to prepare custom monomers by simple and scalable reaction pathways from cheap commercially available starting materials opens the way for the large diffusion of these materials.

In this communication, we explore acrylate-based LCN film biocompatibility by testing their ability to promote cell differentiation and maturation for different murine and human cell lines. We demonstrated how any particular coating or structuration of the material is needed to reproduce results obtainable with more complex cell substrates (e.g., nanostructured surfaces or porous matrix). Interestingly, we demonstrate also that LCN films help human induced pluripotent stem cell-derived cardiomyocyte (hiPSC-CM) growth, speeding it up in respect to common substrates. HiPSC-CMs have typically immature phenotype compared to freshly isolated cardiomyocytes from surgical samples limiting their application in regenerative medicine, disease modeling, and drug testing. The generation of engineered culture substrates has proven to fill the gap with culture on flat surfaces and mimic more closely a physiological cellular microenvironment.[21] Moreover, biomimetic culture systems and time in culture can promote hiPSC-CM with adult-like shape but function that still resemble those of fetal cardiomyocytes.[22] Biomaterial-based culture, such as LCN, may be capable of enhancing and promoting cell maturation as much as possible. This communication represents a powerful preliminary result not only for tissue engineering. In fact, while the advent of soft robotics made by LCNs[3,4] claims for new techniques of noninvasive microsurgery or diagnostics up to reach a single cell, the demonstration of the material biocompatibility is still poorly explored.

The materials explored are LCN films easily and quickly prepared by photopolymerization after alignment of the monomeric compounds in a standard liquid crystalline cell as depicted in **Figure 1**A. The molecular structures of monomers used and the mixture composition are shown in Figure 1B. Compounds **1** and **2** are liquid crystalline molecules that ensure formation of monodomain samples. Molecule **2** acts also as crosslinker leading to the network formation during the polymerization. This architecture is responsible for the mechanical properties of the LCNs and their nonsolubility in common solvents. The material prepared is noted here as MMx, where x (10 or 20) represents the percentage mol/mol of the monomer **2** in the final mixture. **Irgacure 369** (compound **3**) was added in 1% mol/mol to induce the polymerization process by UV light.

Mesomorphic properties of the mixtures were studied by differential scanning calorimetry (DSC) and polarized optical microscopy (POM). MM10 melts directly in the isotropic phase at 53 °C and, only on cooling, a nematic phase was observed. By increasing the crosslinker percentage, the nematic phase becomes enantiotropic and the clearing temperature increases up to 65 °C. The mesophases are easily assigned as nematic by

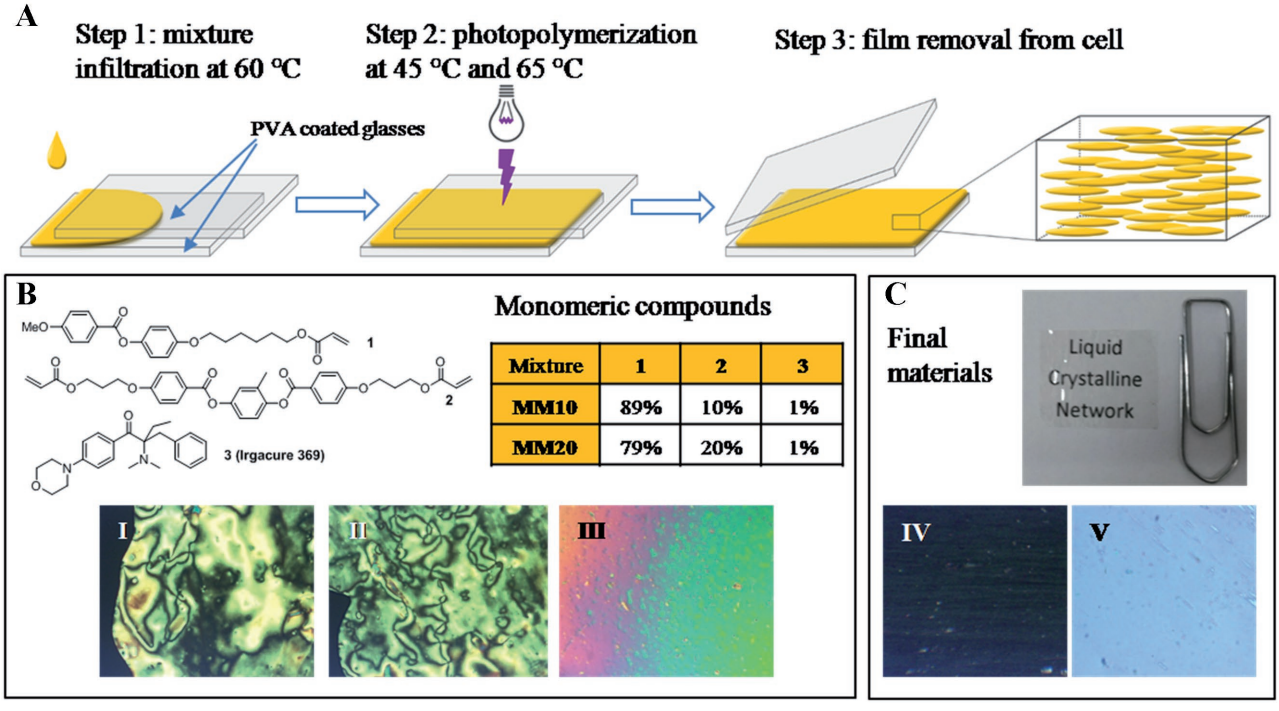

Figure 1. LCN films fabrication. A) Scheme representing the different steps needed for the preparation of LCN with homogeneous planar alignment. B) Monomeric mixtures. Molecular structures, mixture composition, and related POM images. Schlieren nematic textures of mixture MM10 at 45 °C (I) and MM20 at 60 °C on cooling (II) and a marble like texture of MM20 at 50 °C (III). C) Picture of a piece of MM20 film and its POM images with the alignment direction parallel (IV) or at 45° (V) in respect of the analyzer.

the typical Schlieren textures with four- and two- brush defects in POM observation (Figure 1B). Complete mixture characterization is reported in Table S1 and Figure S1 in the Supporting Information.

To prepare the cell scaffolds, the mixtures were melted in the isotropic phase and infiltrated in a liquid crystalline cell for homogeneous alignment. Then, the samples were cooled down at 45 °C until the formation of a monodomain texture and polymerized by irradiation with an UV Light Emitting Diode (LED) lamp. This reaction causes also the retention of the initial LC alignment in the final material, as confirmed by the extinction of the transmission under POM by rotation of the sample every 45° (Figure 1C).

After detachment from the cell glasses, the complete polymerization was checked by Attenuated Total Reflectance (ATR) spectroscopy (Figure S2, Supporting Information) and film thermal properties were studied by DSC. The analysis (full trace reported in Figure S3, Supporting Information) showed similar glass transition temperatures (T_g) for both samples (30 and 32 °C respectively for MM10 and MM20). Clearing temperatures were not observed by DSC and they were difficult to attribute also by POM that showed birefringence of the polymers above 150 °C.[16,23] Scanning Electron Microscope (SEM) images reveal the absence of pores while some surface defects are observed and probably results from the mixture shaping at the interface with the rubbed sacrificial layer (Figure S4, Supporting Information).

Measurement of the order parameter (S) by optical method indicates that both films have the same degree of orientational order showing similar value of S (0.48 and 0.53 respectively for MM10 and MM20, see Figure S5, Supporting Information). The two materials differ only in the mechanical properties, with MM20 more rigid than MM10, as already reported[16] and further demonstrated by the passive tensions measurements described in Figure S6 in the Supporting Information.

The film fabrication does not require organic solvents (only water is needed for the glass coating) or other toxic compounds figuring out as a very simple and safe protocol, easily reproducible also in not well equipped laboratory.

The LCN films exhibit shape change behavior under heating and, in particular, they are able to contract along the alignment direction. However, modifying the bottom coating in the polymerization cell allows to obtain different alignments which results in different deformations such as bending or torsion (Figure S7, Supporting Information).

To evaluate the biocompatibility of LCN films for eukaryotic cells, adhesion tests were carried out using both human dermal fibroblasts (HDFs) and an immortalized mouse myoblast cell line (C2C12). LCN films (0.5 cm x 1.0 cm) were used as prepared or after a washing treatment (subsequent baths in mixtures of hexane and toluene to eliminate impurities not bounded to the network, followed by drying) and with or without poly-L-lysine coating. After, C2C12 cells were directly seeded on the LCN film (about 25.000 cells on MM20 or MM10). To evaluated whether cells adhere or not onto LCNs, 24 h after seeding the films were observed to contrast phase microscopy. No differences were observed between washed or unwashed, coated or uncoated films in terms of cell adhesion (Figure S8, Supporting Information). For this reason, films prepared without the need of any treatment were used in the following tests. Analysis with contrast phase microscopy evidenced how, after 24 h from seeding (**Figure 2**A,C,E,G), LCNs were widely populated by cells showing a round nucleus and an elongated shape as usually shown by C2C12 and HDF cells on Petri dishes (Figure 2I,L).

Further tests were carried out to evaluate the ability of C2C12 and HDF cells to proliferate in adhesion onto our supports. Cells were seeded on LCNs and incubated at 37 °C in the presence of 5% CO_2 and growth medium for 6 d. At the end of sixth day, cell density on films was evaluated by contrast phase microscopy. We found that in all LCNs tested, C2C12 and HDF cells proliferated until the confluence (Figure 2B,D,F,H), confirming that these LCNs represent a good growing layer for both murine and human cells.

Interestingly, after 7 d incubation, significant differences in term of cell alignment were observed between MM20 and MM10 LCN films and HDF grown on Petri dishes. In particular, HDFs grown on MM20 films appeared clearly aligned, whereas those grown on MM10 films show a lower degree of alignment (**Figure 3**A,B). On the contrary, HDF seeded on Petri dishes grown without any preferred orientation (Figure 3C), thereby highlighting a cell orienting ability of LCN films in dependence of their composition. Importance of mechanical properties of the LC scaffolds in HDF alignment was already observed,[24] and our example confirmed as the more rigid material represents a high performance substrate for cell culture.

Similar results were obtained using C2C12 cells. In fact, myoblasts grow randomly onto Petri dishes (Figure 3F) and MM10 films (Figure 3E), whereas muscle cells growing on MM20 films appeared globally aligned (Figure 3D). However, cells' orientation is not clearly showing a correspondence with the homogeneous unidirectional alignment presented by the LC order, as demonstrated by low magnification images in Figure S9 in the Supporting Information.

Finally, the ability of C2C12 cells to undergo differentiation after adhesion onto LCNs was evaluated. C2C12 cells were seeded on MM20 film and grown until 70% confluence. Then, cells were incubated in the presence of differentiation medium, to allow the conversion of myoblasts into myotubes. After 2 d incubation, films were withdrawn and cells stained to analyze their morphology and alignment degree. We observed that C2C12 cells are clearly aligned on the film surface, making end-to-end, and lateral cell contacts during the early phases of differentiation process, confirming that films promote cell alignment and fusion (Figure S10, Supporting Information).

To confirm that C2C12 cells adherent onto MM20 films undergone differentiation, further tests were carried out. Cells seeded onto MM20 films are incubated with differentiation medium for 15 d. Then, cells were fixed, and stained with phalloidin, and Hoechst dye to visualize actin fibers, and cell nuclei. All samples were analyzed using a confocal microscope. We found C2C12 cells grown onto MM20 films form multinucleated myotubes showing well-organized actin fibers with anisotropic alignment (**Figure 4**). We can speculate that the previously highlighted cell alignment on MM20 (Figure 3D) helps cell differentiation promoting more organized and aligned fibers than on other substrates.

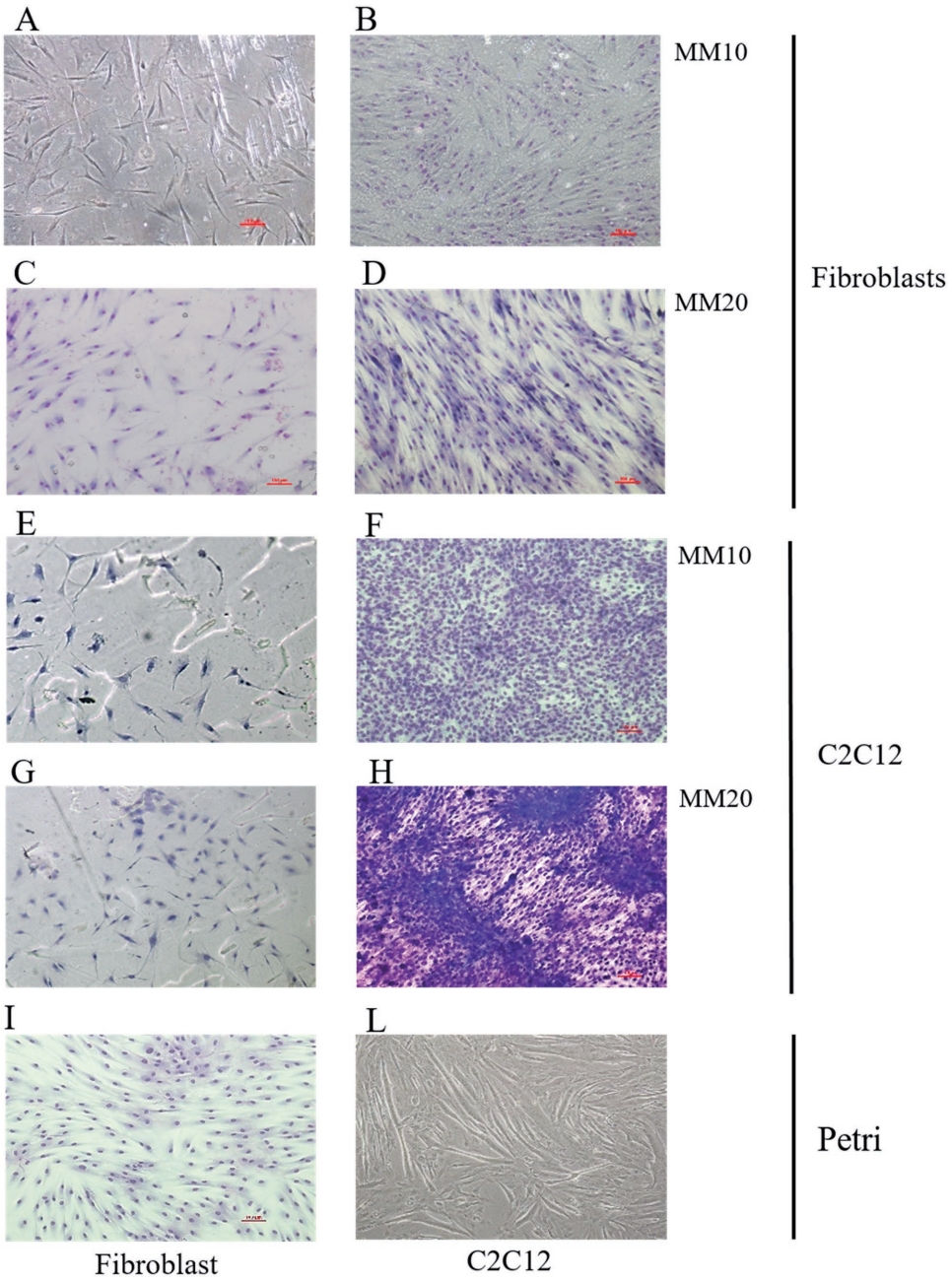

Figure 2. Adhesion and proliferation tests. Phase contrast microscope analysis of HDF and C2C12 adherent on MM10 (images (A,B) and (E,F), respectively), MM20 (images (C,D) and (G,H), respectively), and Petri dishes (images (I) and (L), respectively) at different times. Images (A), (C), (E), and (G) are recorded after incubation at 37 °C in a humidified, CO_2-controlled atmosphere for 24 h. Images (B), (D), (F), (H), (I), and (L) are recorded after incubation of the LCN samples (or petri dishes for (I) and (L)) hosting adherent cells for further 6 d in the presence of growth medium (every 2 d the medium were withdrawn and substituted with fresh one). All images are recorded with a 10× magnification (scale bar: 100 µm). Cells are stained using Diff-Quik Kit.

Similarly, also C2C12 cells grown onto MM10 film generated well-defined myotubes after 15 d differentiation, containing mature actin fiber structures, as revealed by immunostaining with Rhodamine-conjugated phalloidin (Figure S11, Supporting Information). However, the number of mature myotubes found on these films was almost undetectable, suggesting that MM10 films are less performing than the MM20 films in favoring muscle cells alignment and differentiation. These evidences agree with above results showing that C2C12 myoblast show a poor alignment once seeded on MM10 film (Figure 2G) and confirm how material composition plays an important role in the ability of the films to promote cell differentiation.[8] In particular, we have highlighted how important features to be considered when preparing LCN cell substrates are the mechanical properties that depends, in these examples, from the crosslinker percentage.[16] Thus resulting in MM20

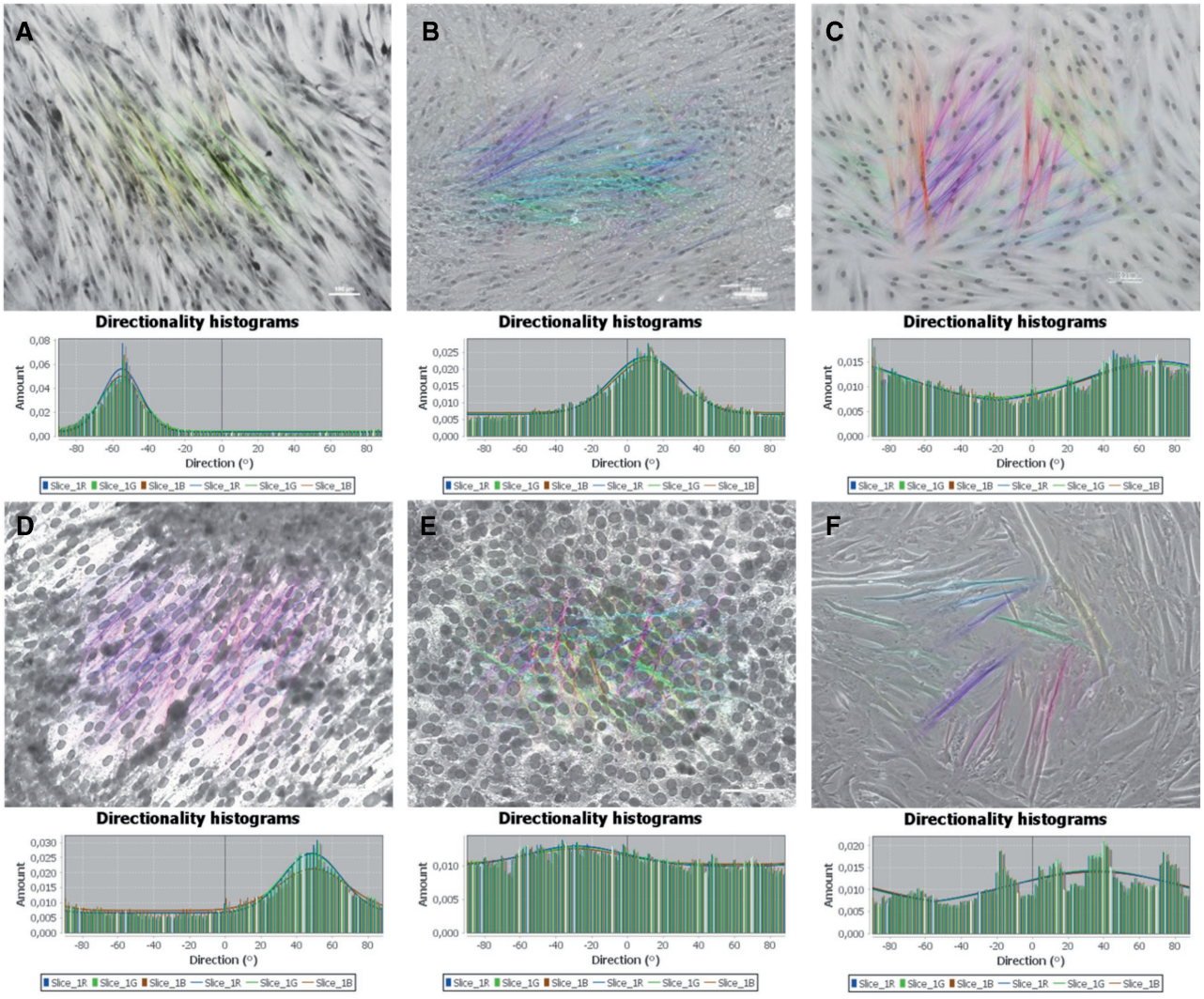

Figure 3. Calculated directionality of HDF and C2C12 on different substrates. Orientation maps and directionality histograms obtained by imageJ (directionality plugin, angles refer to the perpendicular in the middle point of the image) on phase contrast microscopy images of cells (HDF and C2C12) seeded on LCN membranes for 7 d and stained using Diff-Quik Kit (20× lens magnification). A) HDF on MM20; B) HDF on MM10; C) HDF on Petri dish; D) C2C12 on MM20; E) C2C12 on MM10; and F) C2C12 on Petri dish. Superiority of MM20 as substrate for cell alignment is highlighted by the histograms.

as a better platform for the attachment and proliferation of C2C12.

Together our results suggest that LCN films guide cells orientation and differentiation, thereby contributing generation of transversal cell–cell contacts. In contrast, myotubes obtained from C2C12 cells seeded on Petri dishes appeared larger in dimension and randomly distributed (Figure 2L).

On the basis of the proved biocompatibility of the materials, we envisaged that LCN scaffold may provide a suitable platform for tissue engineering and a more physiological microenvironment for disease modeling. We hence evaluated hiPSC-CMs interacting with uncoated LCN MM20 substrates and how this biomaterial may affect cell maturation compared to normal plastic-based flat surfaces. Low density cultures were analyzed in order to better evaluate the cell growth and dimensions. Single human iPSC-derived cardiomyocytes (hiPSC-CMs) of about 30 d postdifferentiation were cultured at low density onto uncoated LCNs for additional 30 d after thawing and observing for cell spreading. 24 h after plating, hiPSC-CMs were capable to adhere and spread onto LCN surface. Between 5 and 7 d after thawing, hiPSC-CMs were typically small and round-shaped, exhibited spontaneous beating but were able to mature over the course of 30 d onto LCNs (**Figure 5**A). Compared to the 5 d counterparts, 30 d hiPSC-CMs were more rod-shaped showing increased cell area, perimeter, cell length but shorter diameter. Moreover, increased cell dimensions dramatically decreased the circularity index, overall indicating that LCN can favor a more mature cell phenotype in a short period of culture (Movie S1, Supporting Information). In addition, we compared cell dimensions with age-matched hiSPC-CMs cultured onto coverslips with flat surface (30 d). HiPSC-CMs showed overall widespread cell area and perimeter due to increased cell length and diameter but had still higher circularity index. We additionally recorded action potentials (APs)

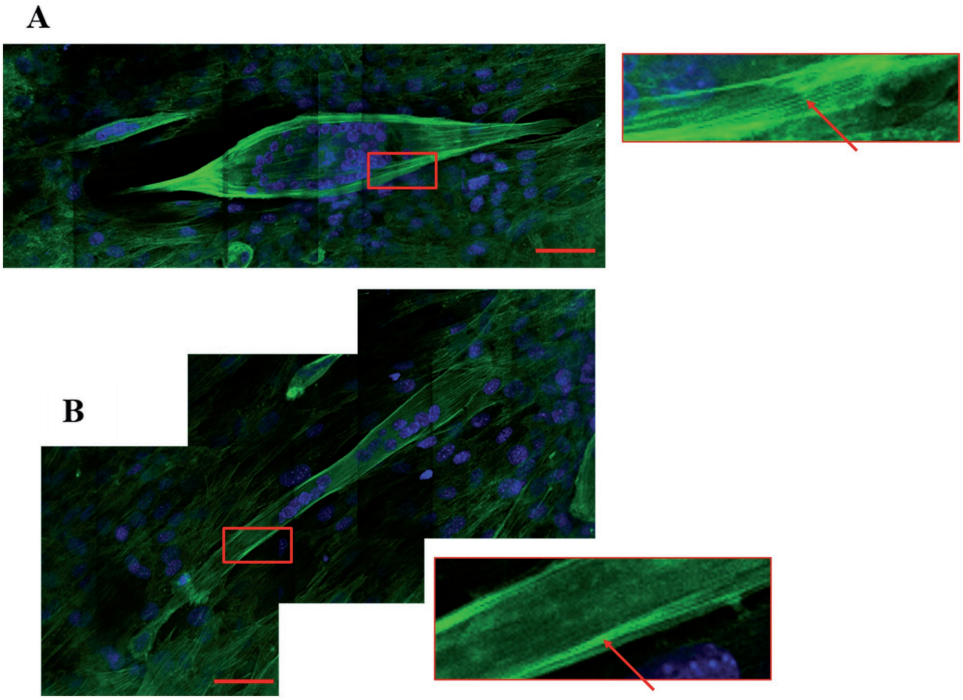

Figure 4. Differentiated C2C12 cells adherent onto LCN film. C2C12 cells seeded onto MM20 LCN films, grown until 70% confluence and then treated by growth medium containing 2% horse serum to induce cell differentiation. Images are recorded by confocal microscopy after cell incubation with Fluorescein isothiocyanate labeled phalloidin (FITC-phalloidin) for 20 min in the dark and with Hoechst 33342 to stain nuclei. A,B) Example of myotubes grown onto MM20 films (scale bar: 50 µm). The regions in the red box of (A) and (B) are shown magnified and show well-aligned F-actin fibers.

to test the functionality of hiPSC-CMs onto LCNs. HiPSC-CMs exhibited spontaneous cardiac-type action potentials (Figure 5B). 30 d hiPSC-CMs stimulated at 1 Hz (Figure 5C) showed hyperpolarized maximal diastolic potential (MDP, –72.7 ± 4 mV), large amplitude (94.6 ± 9.4 mV), and action potential duration (APD90, 125.4 ± 28.9 ms) suggesting integrity of membrane potential and possibility to develop a more mature cardiac phenotype onto LCNs.

In summary, we demonstrated that by a simple and quick process it is possible to prepare acrylate-based LCNs showing biocompatibility for both murine and human cells. By seeding murine muscle cells (C2C12) and HDF we demonstrated complete adhesion on bare films and differentiation for muscular cells. C2C12 differentiate in long muscle fibers showing several nuclei and well organized actin fibers. Different degrees of cell alignment were highlighted due to film composition, and we can speculate that it depends from their rigidity. Furthermore, seeding single human iPSC-derived cardiomyocytes we demonstrated the advantage of LCN for the obtainment of more mature cardiac phenotype in a short period of culture, maintaining the integrity of film action potential.

The demonstrated versatility of LCNs toward different cell lines and their intrinsic properties (e.g., the ability to support stress and to change their shape reversibly by application of different external stimuli) opens to dynamic cell culturing promoting and driving cell differentiation and maturation toward engineered heart and skeletal muscular tissues. Thus, opening to new techniques for regenerative medicine and to fabricate bioartificial muscles to replace and repair at the injury sites.

Experimental Section

General Procedure and Materials: Molecules **1** and **2** were purchased by Synthon Chemical, Irgacure 369 was purchased from Sigma-Aldrich. Thermal transitions were measured using a DSC TA Instruments Q-2000 calorimeter under a nitrogen atmosphere (heating and cooling rate: 10 °C min^{-1}). POM was performed using an inverted microscope (Zeiss, Axio Observer A1) with crosspolarizers and fitted with a Linkam PE120 hot stage. A scanning electron microscope (PHENOM-World) was used to observe the film surfaces after sputter coating them with a 10 nm gold layer. Infrared (IR) spectra were recorded with a Fourier transform (FT) Perkin-Elmer Spectrum BX FT-IR System spectrophotometer. Polarized UV–vis spectra were recorded by a Cary-4000 Varian spectrophotometer equipped with a linear polarizer sheet.

LCN Film Preparation: Liquid crystalline cells were prepared by means of two poly(vinyl alcohol) (PVA) coated glasses rubbed with a velvet cloth and 20 µm glasses spheres as spacers. The coating was chosen in order to reach the homogeneous planar alignment of the mixtures. The monomer mixtures were melted on a hot plate at 60 °C and then infiltrated for capillarity in the cells. Afterward, the samples were cooled down until 45 °C and irradiated for 10 min with an UV LED lamp (Thorlabs M385L2-C4, 385 nm, I = 1.8 mW cm^{-2}). Then, cells were heated at 65 °C and irradiated for further 10 min. After polymerization, cells were opened and the films were removed.

Biological Essay: The films were sterilized and placed in 35 mm Petri dishes. Then, about 25.000 cells were directly seeded on coated or uncoated LCN films (MM20 or MM10) and stored under standard cell culture conditions for 24 h. After this time, LCNs were transferred in new dishes, washed with phosphate-buffered saline (PBS), and stained using Diff-Quik Kit. The presence of C2C12 (or HDF) adherent cells on LCNs was evaluated using the contrast phase microscope. Film coating was carried out using a poly-L-lysine solution. Briefly, poly-L-lysine solution was diluted 1:10 in steril PBS solution, filtered using 0.22 µm filters, and then added to petri dishes containing LCN films. Films were completely covered with the solution and stored at room

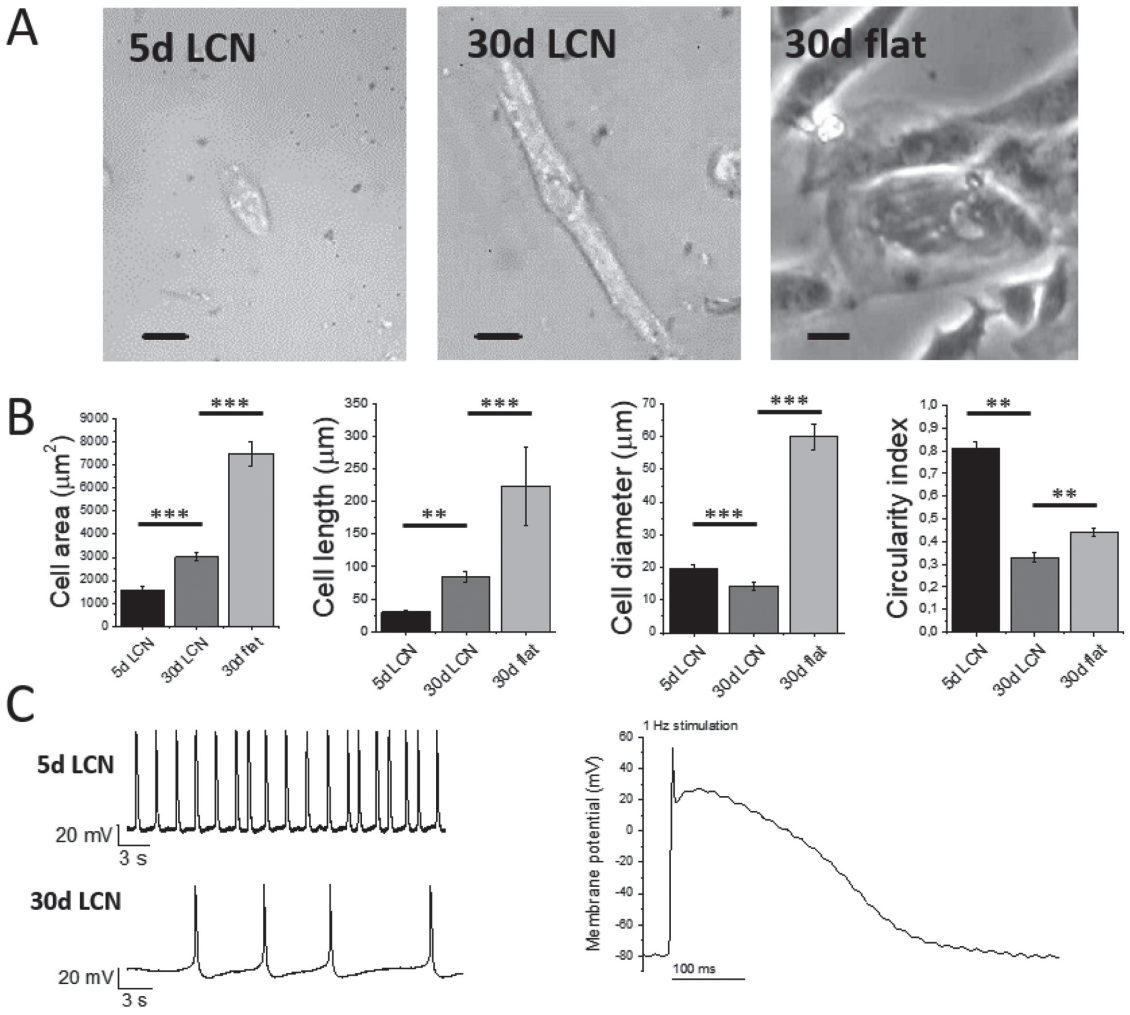

Figure 5. Attachment and maturation of human induced pluripotent stem cell-derived cardiomyocytes (hiPSC-CMs) onto LCNs. A) Representative images of hiPSC-CMs 5 d after plating onto an uncoated LCN (5 d LCN, left), 30 d after plating onto an LCN (30 d LCN, center) and 30 d after plating onto a flat surface (30 d flat, right). B) Comparison of the shape and dimension of hiPSC-CMs grown on uncoated LCNs (5 and 30 d after plating) with cells grown on flat surfaces. From left to right: cell area, cell length, cell diameter, and circularity index. Means ± standard error from 20 cells/2 plates (5 d LCE), 41 cells/2 plates (30 d LCE), 46 cells/2 plates (30 d flat); $^{**}p < 0.01$ and $^{***}p < 0.0001$ estimated by one-way Analysis of Variance (ANOVA) with Tukey post hoc test. C) Left: Representative membrane voltage traces recorded with patch-clamp in unstimulated current-clamp configuration from hiPSC-CMs grown on LCE at 5 d (top) and 30 d (bottom) after plating: spontaneous beating rate markedly reduced over 30 d. Right: Representative trace of a cardiac-type action potential elicited at 1 Hz exhibited by a hiPSC-CM plated on an LCN after 30 d.

temperature for 1 h. Polylysine solution was removed before cell seeding.

For differentiation tests C2C12 cells were seeded onto MM20 LCN films and grown until these reached 70% confluence. Then, growth medium containing 2% horse serum was added to induce cell differentiation. Every 3 d, fresh growth medium was added to dishes containing LCN films. After 20 d, all films were withdrawn, washed with PBS, and incubated with fixing solution (4% paraformaldehyde) for 15 min at room temperature. After, fixing solution was removed and cells were permeabilized using a solution containing 0.1% Triton X-100 for 30 min. Cells were incubated with Alexa FluorH 555 phalloidin for 20 min in the dark. Finally, the films were incubated with Hoechst 33342 to stain nuclei. The slides were left overnight in the dark at room temperature before examination. Stained cells were imaged using Nikon Eclipse TE2000-U (Nikon, Tokyo, Japan) confocal microscopy. A single composite image was obtained by superimposition of ten optical sections for each sample observed. Image size: 212 μm × 212 μm. Images were processed using Photoshop software (Adobe, USA).

Human iPSC-Derived Cardiomyocytes Growth Test: Human iPSC-derived cardiomyocytes of about 30 d postdifferentiation (hiPSC-CMs, ax2505, Axol Bioscience Ltd) were plated onto uncoated sterile LCNs. LCN strips were adhered to a 35 mm of diameter round coverslips, sterilized in 70% ethanol, and PBS washed prior to cell plating. A vial of hiPSC-CMs (1×10^6 cells per vial) was removed from liquid nitrogen storage and thawed rapidly in a 37 °C water bath. HiPSC-CMs (250 000 cells mL^{-1} of cell density) were suspended into Axol Cardiomyocyte Maintenance Medium (ax2530-500) with supplement (Axol Unlock, ax0044) and 10% fetal bovine serum (FBS). A total of 100 μL of cell suspension was added onto each LCN strip resulting in a total of 25 000 cells per LCN and kept overnight in plating medium plus 10% FBS at 37 °C, 5% CO_2. Cells were fed with prewarmed Maintenance Medium plus supplement every other day and monitored for cell growth and action potential at 30 d after thawing (60 d postdifferentiation totally). For cell dimensions, images were acquired by light microscopy using an Evolve 512 Delta camera (Photometrics) and analyzed by Fiji (Image J) plugin. APs of hiPSC-CMs were recorded using the perforated patch whole-cell voltage clamp with amphotericin-B at 37 °C as previously described.[25] For AP recordings,

the pipette solution contained (in $\times 10^{-3}$ M) 115 K methanesulfonate, 25 KCl, 10 (4-(2-hydroxyethyl)-1-piperazineethanesulfonic acid) (HEPES), 3 $MgCl_2$, and cells were perfused with Tyrode buffer containing 1.8×10^{-3} M $CaCl_2$. APs were elicited with short depolarizing stimuli (<3 ms) at 1 Hz of stimulation frequency. Action potentials were analyzed for MDP (mV), amplitude (mV), and action potential duration (ADP90, ms) using the Clampfit 10.7 software (Molecular devices)

Supporting Information

Supporting Information is available from the Wiley Online Library or from the author.

Acknowledgements

The research leading to these results has received funding from the European Research Council under the European Union's Seventh Framework Program (FP7/2007–2013)/ERC grant agreement no. (291349) on photonic micro robotics and from Laserlab-Europe EU-H2020 654148; The authors also thanks Ente Cassa di Risparmio di Firenze (2015/0782 and 2015/0781) and Telethon (grant GGP16191). This research project has been also supported by FAS-Salute ToRSADE project.

Conflict of Interest

The authors declare no conflict of interest.

Keywords

cell scaffolds, fibroblast, human induced pluripotent stem cell-derived cardiomyocytes, liquid crystalline networks, myoblasts

Received: August 2, 2017
Published online: October 17, 2017

[1] G. Wu, Y. Jiang, D. Xu, H. Tang, X. Liang, G. Li, *Langmuir* **2010**, *27*, 1505.
[2] A. M. Flatae, M. Burresi, H. Zeng, S. Nocentini, S. Wiegele, C. Parmeggiani, H. Kalt, D. Wiersma, *Light: Sci. App.* **2015**, *4*, e282.
[3] L. Hines, K. Petersen, G. Z. Lum, M. Sitti, *Adv. Mater.* **2016**, *29*, 1603483.
[4] S. Palagi, A. G. Mark, S. Y. Reigh, K. Melde, T. Qiu, H. Zeng, C. Parmeggiani, D. Martella, A. Sanchez-Castillo, N. Kapernaum, F. Giesselmann, *Nat. Mater.* **2016**, *15*, 647.
[5] H. Zeng, P. Wasylczyk, C. Parmeggiani, D. Martella, M. Burresi, D. S. Wiersma, *Adv. Mater.* **2015**, *27*, 3883.
[6] A. M. Lowe, N. L. Abbott, *Chem. Mater.* **2011**, *24*, 746.
[7] a) D. L. Gin, C. S. Pecinovsky, J. E. Bara, R. L. Kerr, *Functional Lyotropic Liquid Crystal Materials*, Springer-Verlag, Berlin **2007**; b) A. Lancelot, T. Sierra, J. L. Serrano, *Expert Opin. Drug Delivery* **2014**, *11*, 547.
[8] A. Sharma, A. Neshat, C. J. Mahnen, A. d. Nielsen, J. Snyder, T. L. Stankovich, B. G. Daum, E. M. La Spina, G. Beltrano, Y. Gao, S. Li, B.-W. Park, R. J. Clements, E. J. Freeman, C. Malcuit, J. A. McDonough, L. T. J. Korley, T. Hegmann, *Macromol. Biosci.* **2014**, *15*, 200.
[9] A. Agrawal, O. Adetiba, H. Kim, H. Chen, J. G. Jacot, R. Verduzco, *J. Mater. Res.* **2015**, *30*, 453.
[10] R. Langer, J. P. Vacanti, *Science* **1993**, *260*, 920.
[11] C.-H. Li, C. Wang, C. Keplinger, J.-L. Zuo, L. Jin, Y. Sun, P. Zheng, Y. Cao, F. Lissel, C. Linder, X.-Z. You, Z. Bao, *Nat. Chem.* **2016**, *8*, 618.
[12] C. Ohm, M. Brehmer, R. Zentel, *Adv. Mater.* **2010**, *22*, 3366.
[13] T. White, D. J. Broer, *Nat. Mater.* **2015**, *14*, 1087.
[14] a) T. Bera, E. J. Freeman, J. A. McDonough, R. J. Clements, A. Aladlaan, D. W. Miller, C. Malcuit, T. Hegmann, E. Hegmann, *ACS Appl. Mater. Interfaces* **2015**, *7*, 14528; b) Y. Gao, T. Mori, S. Manning, Y. Zhao, A. d. Nielsen, A. Neshat, A. Sharma, C. J. Mahnen, H. R. Everson, S. Crotty, R. J. Clements, C. Malcuit, E. Hegmann, *ACS Macro Lett.* **2015**, *5*, 4.
[15] A. Agrawal, H. Chen, H. Kim, B. Zhu, O. Adetiba, A. Miranda, A. C. Chipara, P. M. Ajayan, J. G. Jacot, R. Verduzco, *ACS Macro Lett.* **2016**, *5*, 1386.
[16] D. Martella, D. Antonioli, S. Nocentini, D. S. Wiersma, G. Galli, M. Laus, C. Parmeggiani, *RSC Adv.* **2017**, *7*, 19940.
[17] G. Kocer, J. t. Schiphorst, M. Hendrix, H. G. Kassa, P. Leclère, A. P. H. J. Schenning, P. Jonkheijm, *Adv. Mater.* **2017**, *29*, 1606407.
[18] H. Zeng, D. Martella, P. Wasylczyk, G. Cerretti, J. C. Gomez Lavocat, C.-H. Ho, C. Parmeggiani, D. S. Wiersma, *Adv. Mater.* **2014**, *26*, 2319.
[19] A. Buguin, M. H. Li, P. Silberzan, B. Ladoux, P. Keller, *J. Am. Chem. Soc.* **2006**, *128*, 1088.
[20] Y. Li, G. Huang, X. Zhang, L. Wang, Y. Du, T. J. Lu, F. Xu, *Biotechnol. Adv.* **2014**, *32*, 347.
[21] A. S. Smith, J. Macadangdang, W. Leung, M. A. Laflamme, D. H. Kim, *Biotechnol. Adv.* **2016**, *35*, 77.
[22] J. M. Pioner, A. W. Racca, J. M. Klaiman, K.-C. Yang, X. Guan, L. Pabon, V. Muskheli, R. Zaunbrecher, J. Macadangdang, M. Y. Jeong, D. L. Mack, M. K. Childers, D.-H. Kim, C. Tesi, C. Poggesi, C. E. Murry, M. Regnier, *Stem Cell Rep.* **2016**, *6*, 885.
[23] H. Shahsavan, S. M. Salili, A. Jákli, B. Zhao, *Adv. Mater.* **2015**, *27*, 6828.
[24] A. Sharma, T. Mori, C. J. Mahnen, H. R. Everson, M. T. Leslie, A. d. Nielsen, L. Lussier, C. Zhu, C. Malcuit, T. Hegmann, J. A. McDonough, E. J. Freeman, L. T. J. Korley, R. J. Clements, E. Hegmann, *Macromol. Biosci.* **2017**, *17*, 1600278.
[25] R. Coppini, L. Mazzoni, C. Ferrantini, F. Gentile, J. M. Pioner, T. Laurino, L. Santini, V. Bargelli, M. Rotellini, G. Bartolucci, C. Crocini, L. Sacconi, C. Tesi, L. Belardinelli, J. Tardiff, A. Mugelli, I. Olivotto, E. Cercbai, C. Poggesi, *Circ.: Heart Failure* **2017**, *10*, e003565.